Jülich-Georgia

M. Döring

C. Hanhart, F. Huang, S. Krewald, U.-G. Meißner, K. Nakayama, D. Rönchen,
Forschungszentrum Jülich, University of Georgia, Universität Bonn

Nucl. Phys. A **829**, 170 (2009), Phys. Lett. B **681**, 26 (2009)

The Jülich model of pion-nucleon interaction

Motivation

- Hadronic reactions provide insight to QCD in the non-perturbative region.
- Intense experimental effort at JLab (Clas), ELSA, MAMI, ...
- Theoretical data analysis required (e.g. EBAC/JLab).

- Chiral Lagrangian of Wess and Zumino.
- Channels πN, ηN; effective $\pi\pi N$ channels σN, ρN, $\pi\Delta$.
- Baryonic resonances up to $J = 3/2$ with derivative couplings as required by chiral symmetry.
- New: KY channels, $J = 5/2,\ 7/2$ resonances, chiral unitary σ meson.

Scattering equation in the JLS basis

$$\langle L'S'k'|T^{IJ}_{\mu\nu}|LSk\rangle = \langle L'S'k'|V^{IJ}_{\mu\nu}|LSk\rangle$$
$$+\sum_{\gamma,L''S''}\int_0^\infty k''^2\, dk''\,\langle L'S'k'|V^{IJ}_{\mu\gamma}|L''S''k''\rangle\,\frac{1}{Z-E_\gamma(k'')+i\epsilon}\,\langle L''S''k''|T^{IJ}_{\gamma\nu}|LSk\rangle$$

T: Amplitude V: Pseudopotential G: Propagator

J: total angular momentum
L: orbital angular momentum
S: total Spin of MB system
I: isospin
$k(k',\, k'')$: incoming(outgoing, intermediate) momentum, on- or off-shell
$\mu(\nu,\,\gamma)$: incoming(outgoing, intermediate) channel $[\pi N,\ \eta N,\ \pi\Delta,\ \rho N, \sigma N]$

Scattering equation in the JLS basis

$$\langle L'S'k'|T^{IJ}_{\mu\nu}|LSk\rangle = \langle L'S'k'|V^{IJ}_{\mu\nu}|LSk\rangle$$

$$+\sum_{\gamma,L''S''}\int_0^\infty k''^2\,dk''\,\langle L'S'k'|V^{IJ}_{\mu\gamma}|L''S''k''\rangle\,\frac{1}{Z-E_\gamma(k'')+i\epsilon}\,\langle L''S''k''|T^{IJ}_{\gamma\nu}|LSk\rangle$$

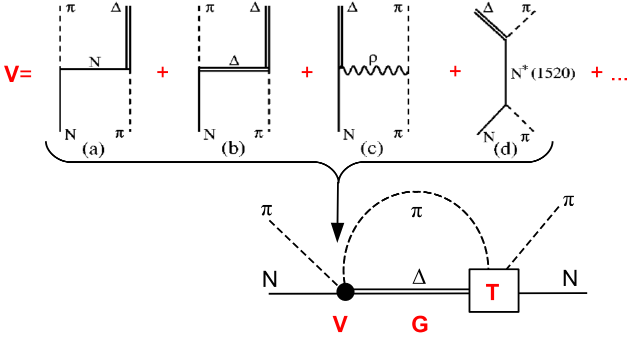

Scattering equation in the JLS basis

$$\langle L'S'k'|T^{IJ}_{\mu\nu}|LSk\rangle = \langle L'S'k'|V^{IJ}_{\mu\nu}|LSk\rangle + \sum_{\gamma,L''S''} \int_0^\infty k''^2\, dk'' \langle L'S'k'|V^{IJ}_{\mu\gamma}|L''S''k''\rangle \frac{1}{Z - E_\gamma(k'') + i\epsilon} \langle L''S''k''|T^{IJ}_{\gamma\nu}|LSk\rangle$$

Other approaches [On-shell factorization of V]

- Omit real part of k" integration $\Rightarrow$ K-matrix approach.
  Unitarity implemented but analyticity from dispersive (real) parts is lost.
  - Retain Lagrangian structure $\Rightarrow$ Giessen model [has extra channels].
  - Model background V^{NP} (= everything except s-channel resonances) by subthreshold resonances $\Rightarrow$ CMB type models.
  - Model V by energy dependent polynomials in each partial wave $\Rightarrow$ GWU (SAID) analysis. However: has constraints from dispersion relations.
- Replacement of meson exchange by chiral contact terms (Weinberg-Tomozawa + maybe NLO) $\Rightarrow$ chiral unitary models.
  Usually restricted to one partial wave, mixing of partial waves through u, t channel exchange is lost.

Partial waves in $\pi N \to \pi N$ (Solution 2002)

"Data": GWU/SAID analysis, single energy solution

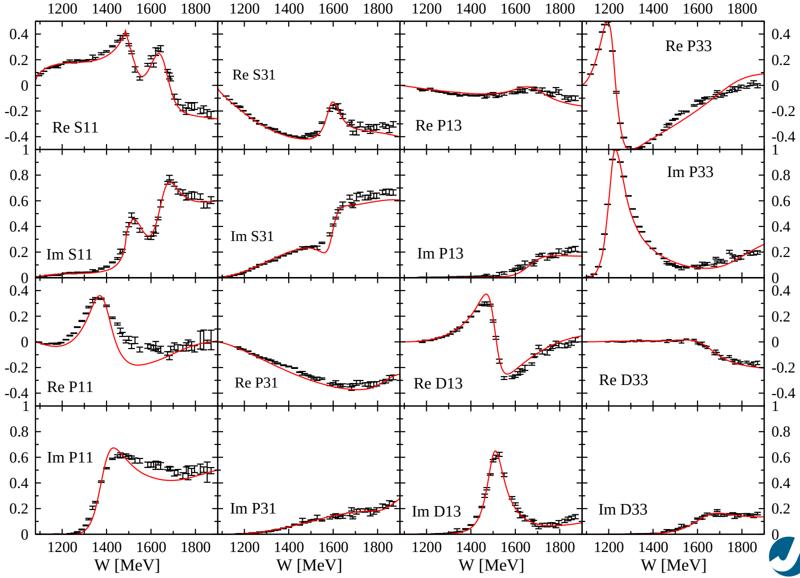

Partial waves in $\pi N \to \pi N$ (Solution 2002)

"Data": GWU/SAID analysis, single energy solution

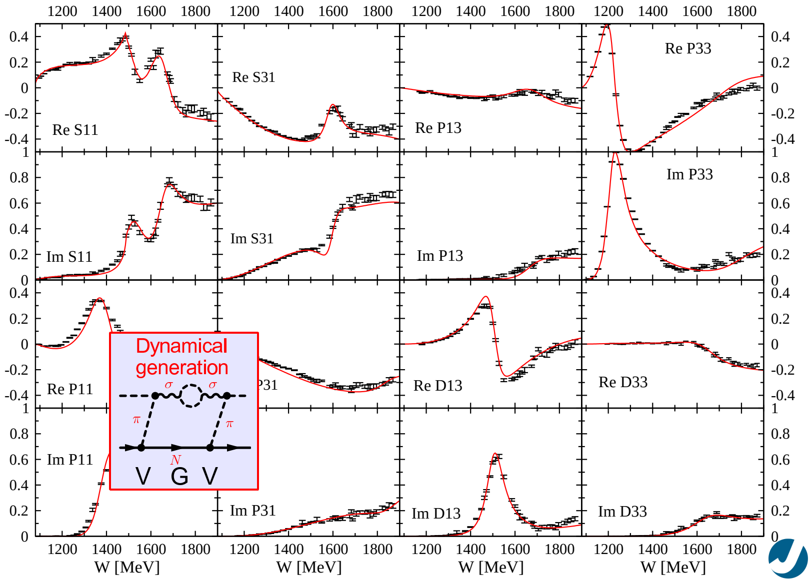

Coupled channel effects in $\gamma N \to \eta N$

[M.D., K. Nakayama, EPJA43 (2010), PLB683 (2010)]

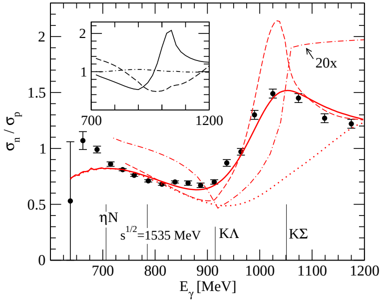

[Data: I. Jaegle et al., CBELSA/TAPS, PRL 100 (2008)]

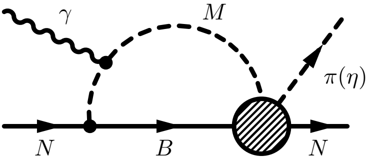

- $MB = \pi N,\ \eta N, K\Lambda, K\Sigma$
- Pronounced cusp from dispersive ("real") part of the loop.
- Analyticity is crucial.

Coupled channel effects in $\gamma N \to \eta N$

[M.D., K. Nakayama, EPJA43 (2010), PLB683 (2010)]

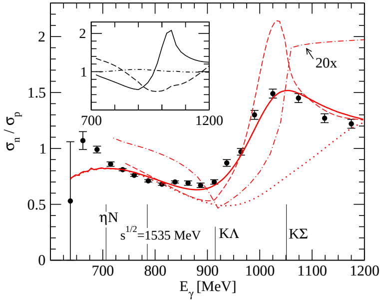

[Data: I. Jaegle et al., CBELSA/TAPS, PRL 100 (2008)]

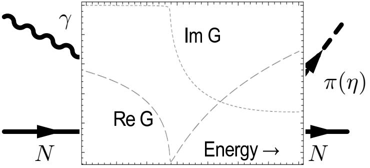

- $MB = \pi N,\ \eta N, K\Lambda, K\Sigma$
- Pronounced cusp from dispersive ("real") part of the loop.
- Analyticity is crucial.

Propagator of stable particles $\pi\pi$, πN, ηN (c.m. system)

$$\Pi_\sigma(z) = \int_0^\infty q^2 dq \, \frac{(v^{\sigma\pi\pi}(q,z))^2}{z - E_1 - E_2 + i\epsilon}$$

$$E_{1,2} = \sqrt{m_{1,2}^2 + q^2}$$

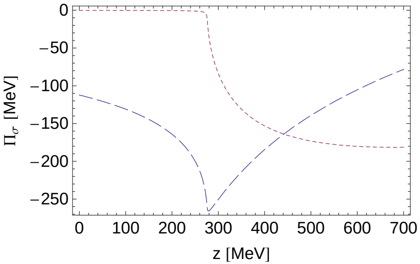

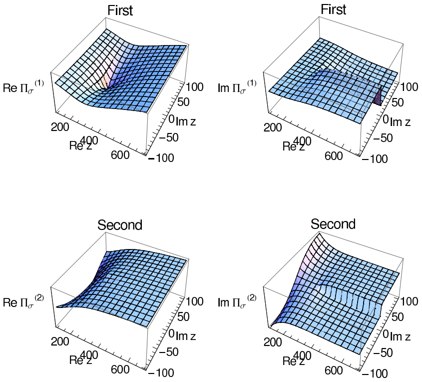

→ Righthand cut, two sheets, and one branch point!

Analytic continuation via Contour deformation

...enables access to all Riemann sheets

$$\Pi_\sigma(z) = \int_0^\infty q^2 dq \, \frac{(v^{\sigma\pi\pi}(q))^2}{z - E_1 - E_2 + i\epsilon}$$

$$z - E_1 - E_2 = 0 \Leftrightarrow q = q_{c.m.}$$

$$q_{c.m.} = \frac{1}{2z}\sqrt{[z^2 - (m_1 - m_2)^2][z^2 - (m_1 + m_2)^2]}$$

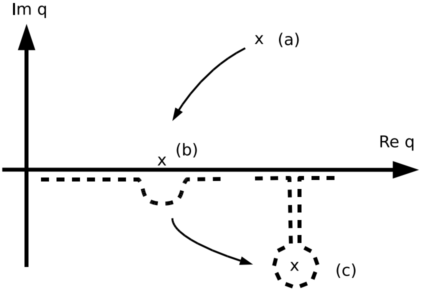

- Plot $q_{c.m.}(z)$ in the q plane of integration (X: Pole positions).
- case (a), Im $z > 0$: straight integration from $q = 0$ to $q = \infty$.
- case (b), Im $z = 0$: Pole is on real q axis.
- case (c), Im $z < 0$: Deformation gives analytic continuation.
- Special case: Pole at $q = 0$ $\Leftrightarrow$ branch point at $z = m_1 + m_2$ (= threshold).

Propagator of effective $\pi\pi N$ channels σN, ρN, $\pi\Delta$

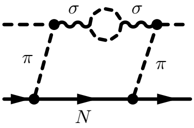

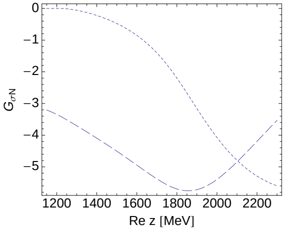

$$g_{\sigma N}(z,k) = \frac{1}{z - \sqrt{m_N^2 + k^2} - \sqrt{(m_\sigma^0)^2 + k^2} - \Pi_\sigma(z_\sigma(z,k),k)},$$

$$G_{\sigma N}(z) = \int_0^\infty dk\, k^2\, F(k)\, g_{\sigma N}(z,k),$$

$$z_\sigma(z,k) = z + m_\sigma^0 - \sqrt{k^2 + (m_\sigma^0)^2} - \sqrt{k^2 + m_N^2}$$

Contour deformation (effective $\pi\pi N$ propagator)

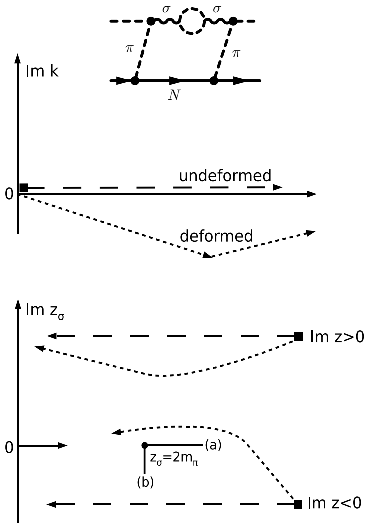

$$\Pi_\sigma^{(b)} = \begin{cases} \Pi_\sigma^{(2)} & \text{if Im } z_\sigma < 0 \\ & \text{and Re } z_\sigma > 2m_\pi \\ \Pi_\sigma & \text{else} \end{cases}$$

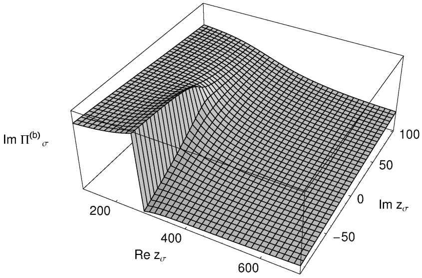

Analytic structure from the $\pi\pi N$ cut

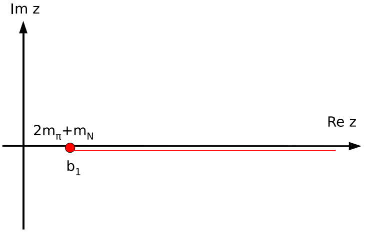

- The cut along Im $z = 0$ from $z = 2m_\pi + m_N$ to ∞ is induced by the cut of the self energy of the unstable particle.
- The analytic continuation along this cut is obtained by contour deformation of the k integration ("σN loop") and simultaneous rotation of the cut of the σ self energy.

- Continuation at fixed Re z's:

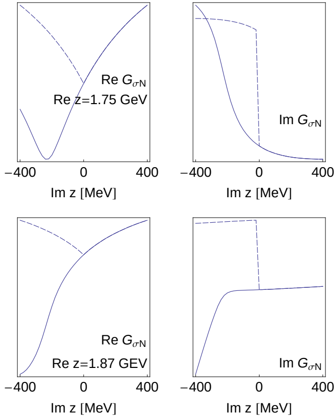

$\rightarrow$ Branch point in the complex z plane.

Branch points in the complex plane

$$\frac{1}{z-\sqrt{m_N^2+k^2}-\sqrt{(m_\sigma^0)^2+k^2}-\Pi_\sigma(z_\sigma(z,k),k)}$$

denominator can become zero (pseudo-two-body singularity).

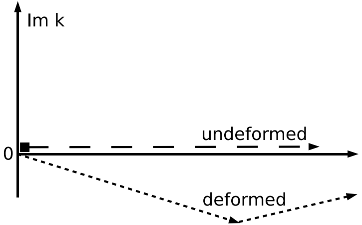

- Pseudo-two-body singularity can be passed ”left” or ”right”.
- Contours $\Gamma^{(2)}$ and $\Gamma^{(3)}$ distinguish the new Riemann sheets.
- Choice of $\Gamma^{(2)}$ and $\Gamma^{(3)}$ for every z defines the position of the associated cut.
- New branch points in the complex plane.

Branch points in the complex plane

$$\frac{1}{z-\sqrt{m_N^2+k^2}-\sqrt{(m_\sigma^0)^2+k^2}-\Pi_\sigma(z_\sigma(z,k),k)}$$

denominator can become zero (pseudo-two-body singularity).

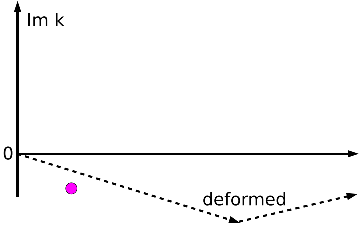

- Pseudo-two-body singularity can be passed "left" or "right".
- Contours $\Gamma^{(2)}$ and $\Gamma^{(3)}$ distinguish the new Riemann sheets.
- Choice of $\Gamma^{(2)}$ and $\Gamma^{(3)}$ for every z defines the position of the associated cut.
- New branch points in the complex plane.

Branch points in the complex plane

$$\frac{1}{z - \sqrt{m_N^2 + k^2} - \sqrt{(m_\sigma^0)^2 + k^2} - \Pi_\sigma(z_\sigma(z,k),k)}$$

denominator can become zero (pseudo-two-body singularity).

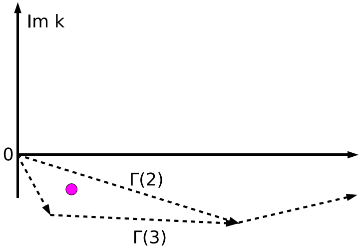

- Pseudo-two-body singularity can be passed ”left” or ”right”.
- Contours $\Gamma^{(2)}$ and $\Gamma^{(3)}$ distinguish the new Riemann sheets.
- Choice of $\Gamma^{(2)}$ and $\Gamma^{(3)}$ for every z defines the position of the associated cut.
- New branch points in the complex plane.

Effective $\pi\pi N$ channels: Analytic structure

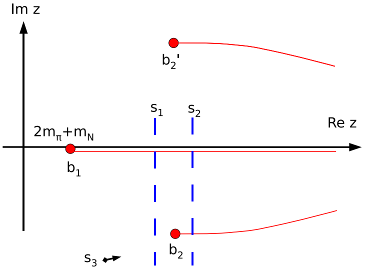

- The cut along Im $z = 0$ is induced by the cut of the self energy of the unstable particle.
- The poles of the unstable particle (σ) induce branch points in the σN propagator at

$$z_{b_2} = m_N + z_0, \; z_{b_2'} = m_N + z_0^*$$

Three branch points and four sheets for each of the σN, ρN, and $\pi\Delta$ propagators.

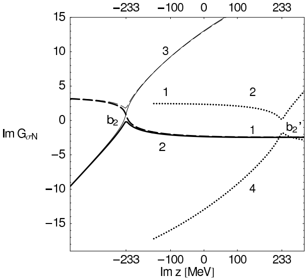

Effective $\pi\pi N$ channels: Analytic structure

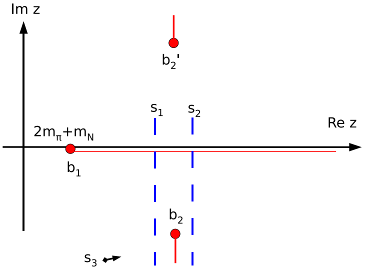

Three branch points and four sheets for each of the σN, ρN, and $\pi\Delta$ propagators.

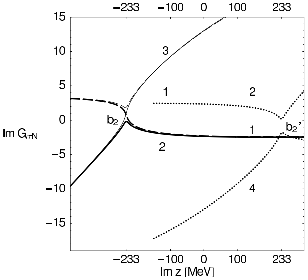

- The cut along Im $z = 0$ is induced by the cut of the self energy of the unstable particle.
- The poles of the unstable particle (σ) induce branch points in the σN propagator at

$$z_{b_2} = m_N + z_0, \; z_{b_2'} = m_N + z_0^*$$

Poles and residues

on the unphysical sheets, given by the analytic continuation.

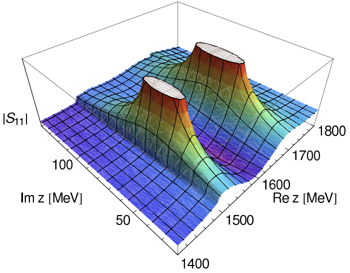

	Re z_0 [MeV]	-2 Im z_0 [MeV]	$\|R\|$ [MeV]	θ [deg] [^{0}]
$N^*(1440)\ P_{11}$	1387	147	48	-64
ARN	1359	162	38	-98
HOE	1385	164	40	
CUT	1375$\pm$30	180$\pm$40	52$\pm$5	-100$\pm$35
$N^*(1520)\ D_{13}$	1505	95	32	-18
ARN	1515	113	38	-5
HOE	1510	120	32	-8
CUT	1510$\pm$5	114$\pm$10	35$\pm$2	-12$\pm$5

	Re z_0 [MeV]	-2 Im z_0 [MeV]	$\|R\|$ [MeV]	θ [deg] [^{0}]
$N^*(1535)\ S_{11}$	1519	129	31	-3
ARN	1502	95	16	-16
HOE	1487			
CUT	1510$\pm$50	260$\pm$80	120$\pm$40	+15$\pm$45
$N^*(1650)\ S_{11}$	1669	136	54	-44
ARN	1648	80	14	-69
HOE	1670	163	39	-37
CUT	1640$\pm$20	150$\pm$30	60$\pm$10	-75$\pm$25
$N^*(1720)\ P_{13}$	1663	212	14	-82
ARN	1666	355	25	-94
HOE	1686	187	15	
CUT	1680$\pm$30	120$\pm$40	8$\pm$12	-160$\pm$30
$\Delta(1232)\ P_{33}$	1218	90	47	-37
ARN	1211	99	52	-47
HOE	1209	100	50	-48
CUT	1210$\pm$1	100$\pm$2	53$\pm$2	-47$\pm$1
$\Delta^*(1620)\ S_{31}$	1593	72	12	-108
ARN	1595	135	15	-92
HOE	1608	116	19	-95
CUT	1600$\pm$15	120$\pm$20	15$\pm$2	-110$\pm$20
$\Delta^*(1700)\ D_{33}$	1637	236	16	-38
ARN	1632	253	18	-40
HOE	1651	159	10	
CUT	1675$\pm$25	220$\pm$40	13$\pm$3	-20$\pm$25
$\Delta^*(1910)\ P_{31}$	1840	221	12	-153
ARN	1771	479	45	+172
HOE	1874	283	38	
CUT	1880$\pm$30	200$\pm$40	20$\pm$4	-90$\pm$30

[ARN]: Arndt et al., PRC 74 (2006), [HOE]: Höhler, πN Newsl. 9 (1993), [CUT]: Cutkowski et al., PRD 20 (1979).

Residues to ηN, σN, ρN, $\pi\Delta$. Zeros. Branching ratios to πN, ηN.

Hidden poles in the S_{11} partial wave

[Data: Arndt et al., FA08, EPJA 35 (2008)]

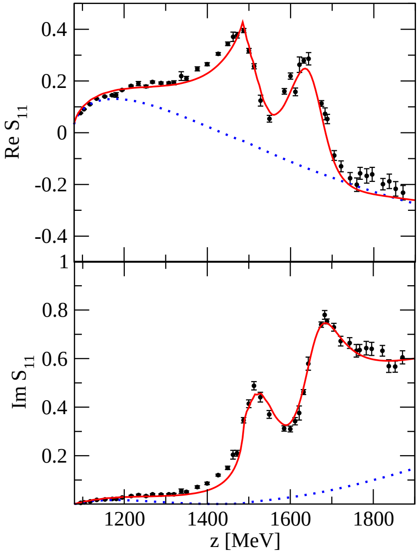

- Laurent series,

$$T^{(2)\,ij} = \frac{a_{-1}^{ij}}{z - z_0} + a_0^{ij} + \ldots$$

- Resonance interference of $N^*(1535)$ and $N^*(1650)$.

Hidden poles in the S_{11} partial wave

[Data: Arndt et al., FA08, EPJA 35 (2008)]

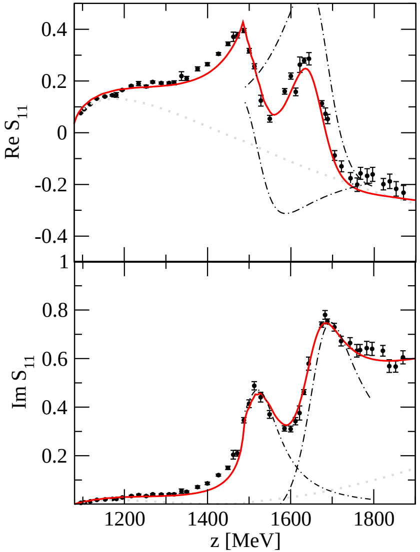

- Laurent series,

$$T^{(2)\,ij} = \frac{a_{-1}^{ij}}{z - z_0} + a_0^{ij} + \ldots$$

- Resonance interference of $N^*(1535)$ and $N^*(1650)$.

JÜLICH FORSCHUNGSZENTRUM

Hidden poles in the S_{11} partial wave

[Data: Arndt et al., FA08, EPJA 35 (2008)]

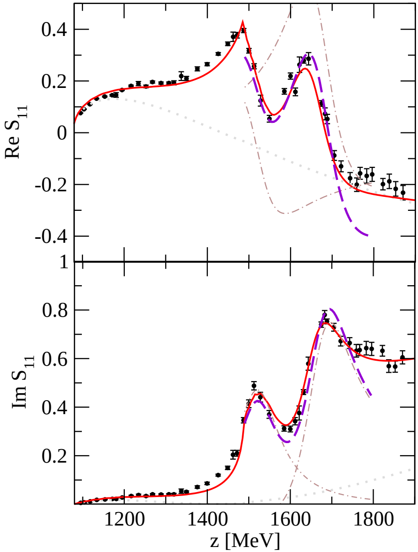

- Laurent series,

$$T^{(2)\,ij} = \frac{a^{ij}_{-1}}{z - z_0} + a^{ij}_0 + \ldots$$

- Resonance interference of $N^*(1535)$ and $N^*(1650)$.

Hidden poles in the S_{11} partial wave

[Data: Arndt et al., FA08, EPJA 35 (2008)]

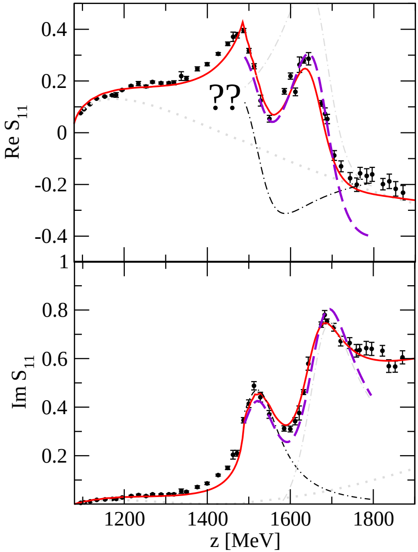

- Laurent series,

$$T^{(2)\,ij} = \frac{a_{-1}^{ij}}{z - z_0} + a_0^{ij} + \ldots$$

- Resonance interference of $N^*(1535)$ and $N^*(1650)$.

Hidden poles in the S_{11} partial wave

[Data: Arndt et al., FA08, EPJA 35 (2008)]

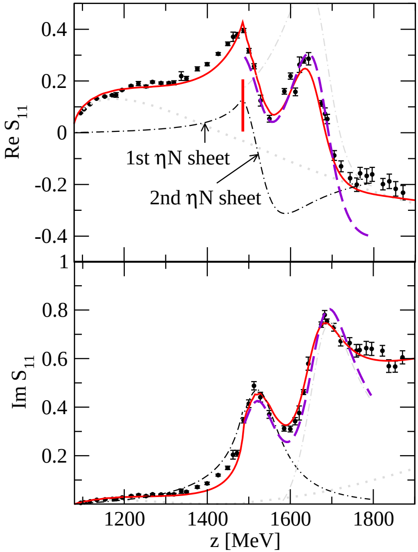

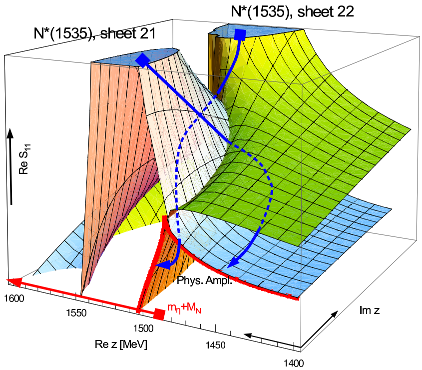

- Different poles on different sheets produce the cusp.

Pole repulsion in P33/D13

Hidden poles in the S_{11} partial wave

[Data: Arndt et al., FA08, EPJA 35 (2008)]

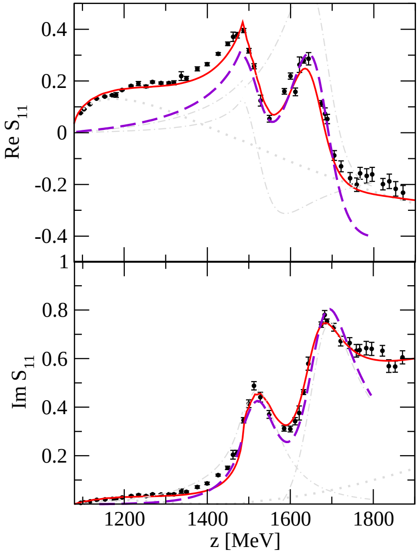

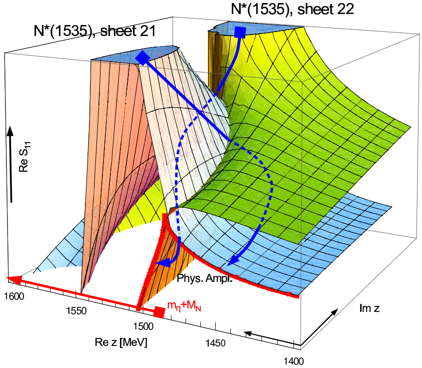

- Different poles on different sheets produce the cusp.

Pole repulsion in P33/D13

JÜLICH FORSCHUNGSZENTRUM

The two poles of the Roper resonance

- SAID/EBAC/Jülich: PRC 69 (2004)/ PRC 79 (2009); arXiv:0909.1356 (2009)/ NPA 829 (2009)]
  two poles of the Roper, in all cases on two different $\pi\Delta$ sheets.
- Poles on hidden sheets can be only seen through the corresponding branch point $\Rightarrow$ Structures from hidden poles appear as...
  - ... cusps if branch point on physical axis ($N(1535)$ case close to ηN threshold)
  - ... washed out cusps (non-standard resonance shape) if branch point in the complex plane (Roper case close to $\pi\Delta$ threshold).
- Proposed two-pole structure of the $\Lambda(1405)$ [Jido et al., NPA 725 (2003); M.D. et al. EPJA 32 (2007)]: both poles on same, non-hidden, sheet $\rightarrow$ experimental tests may be possible.

An additional state in P11

* New pole in P11 found
at z=1620 + 297 i MeV.

——	full ($T^P + T^{NP}$)
– – –	Roper: $a_{-1} / (z-z_0) + a_0$
-·-·-	N(1620): $a_{-1} / (z-z_0)$

* Very weak branching to πN.
* Very large branching to πΔ.
* Resonance transition amplitude
πN --> πΔ:
Manley (πN --> ππN): -0.21
here: -0.25

* Roper: generated from σN.
* N(1620): generated from πΔ.

* Dynamics of the nucleon pole:
Pole repulsion N <--> Roper

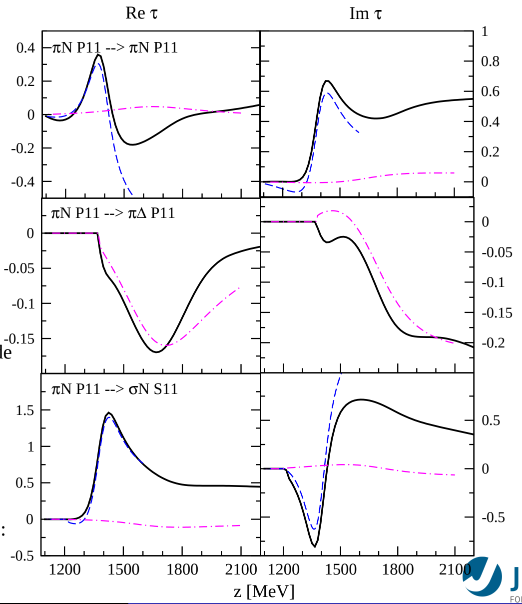

The analytic structure of the P11 partial wave

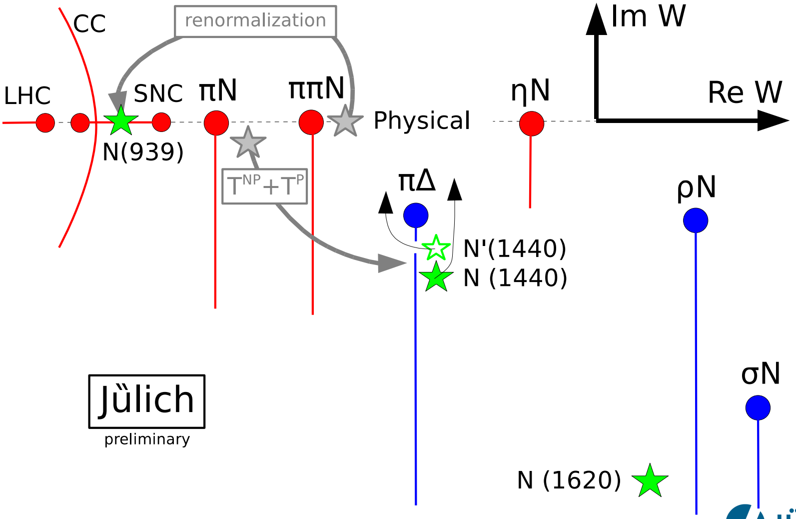

The analytic structure of the P11 partial wave

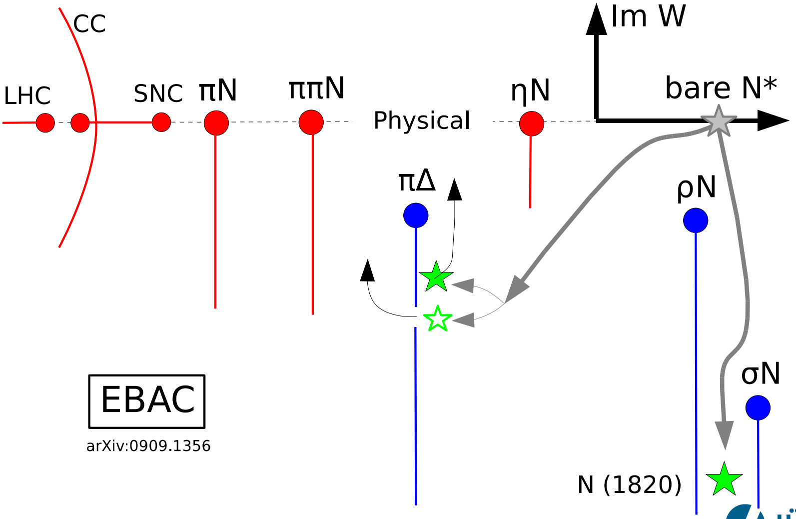

Chiral unitary approach to $\pi\pi$ scattering

$$T_{\pi\pi} = V\chi + V\chi\, G\, T_{\pi\pi}\ ;\ V\chi = \underbrace{(1/2 m_\pi^2 - s)}_{\text{Adler zero}} / f^2$$

$$T_{\pi\pi} = (V_{\sigma\pi\pi})^2 / (z - M - \Sigma_{\pi\pi})$$

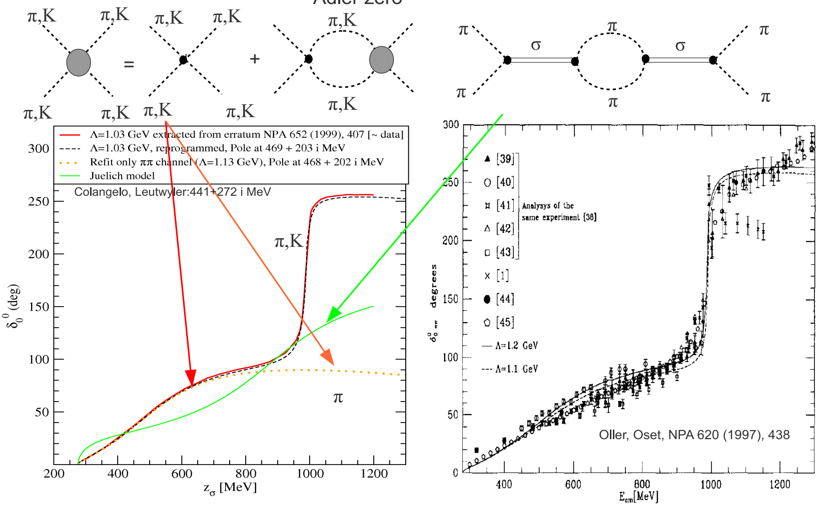

Implementation of the chiral σ

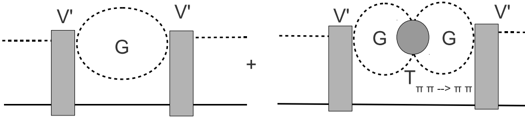

$$G_{sN} = c(z,p)\frac{G(z')}{1 - V(z')G(z')}$$

$$z'^2 = z^2 + m_N^2 - 2z\sqrt{p^2 + m_N^2}$$

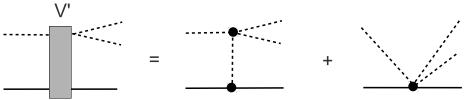

Independence on parameterization
of the pion fields (off-shell cancellatio

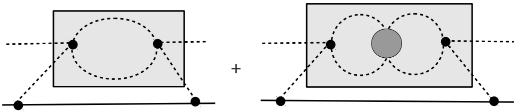

ππ scattering as subprocess
w/o tree level term

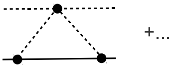

Tree level: Not included (double counting
with ρ, σ t-channel exchanges)

JÜLICH
FORSCHUNGSZENTRUM

Result for the Roper resonance

Readjustment of cut-offs and $g_{\sigma\sigma\sigma}$ coupling

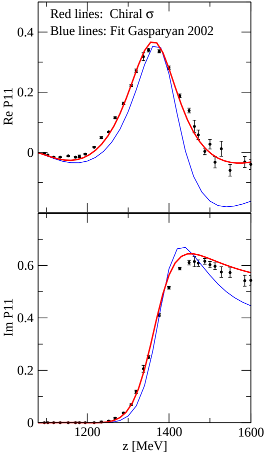

- Analytic structure of the amplitude exactly the same as before (3 branchpoints from σN)
- Dynamical generation of Roper and second P11 does not depend on details of the model
- Chiral σ provides better description.

Result for the Roper resonance

Readjustment of cut-offs and $g_{\sigma\sigma\sigma}$ coupling

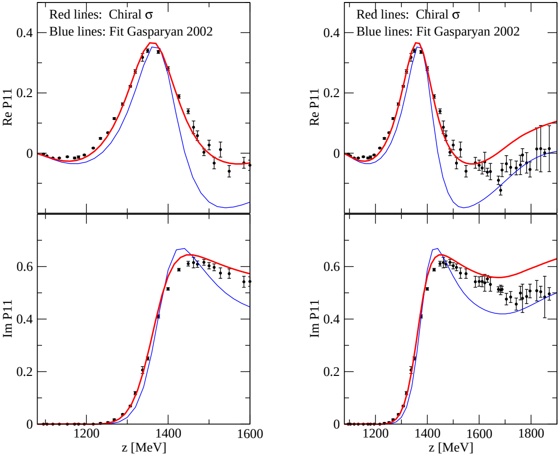

- Analytic structure of the amplitude exactly the same as before (3 branchpoints from σN)
- Dynamical generation of Roper and second P11 does not depend on details of the model
- Chiral σ provides better description.

The reaction $\pi^+ p \to K^+\Sigma^+$

- Pure isospin $3/2$; relatively few Δ resonances.
- $\to$ Strong constraints on the amplitude of the Jülich model!
- Good, simple data situation (Candlin 1983-1988).
- Simultaneous fit to $\pi N \to \pi N$ partial waves plus $\pi^+ p \to K^+\Sigma^+$ observables.
- Requires extended fitting efforts: Parallelization of the code in energies, implementation of Minuit done.
- Code runs on Juropa@Jülich.
- First tasks:
  - Inclusion of KY in $t-$ and $u-$channel exchange processes.
  - Inclusion of Spin 5/2 and Spin 7/2 resonances.

Inclusion of the KY channels

Inclusion via $SU(3)$ symmetry [no additional freedom]

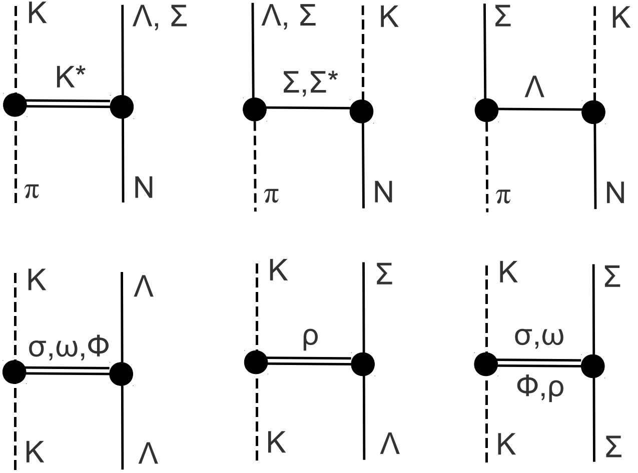

Differential cross section of $\pi^+ p \to K^+\Sigma^+$

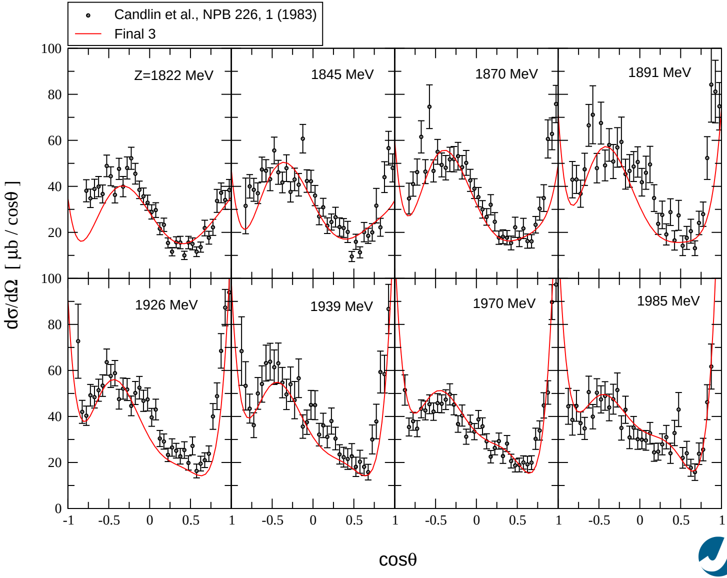

Differential cross section of $\pi^+ p \to K^+ \Sigma^+$

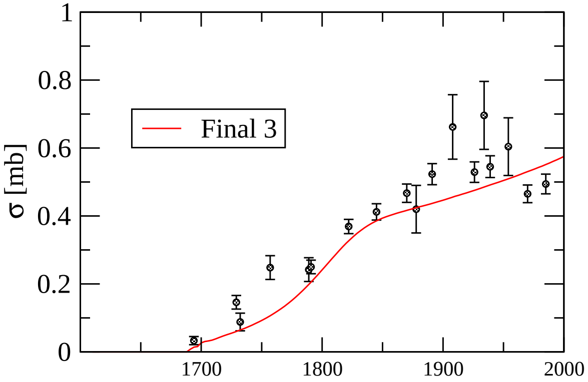

Polarization of $\pi^+ p \to K^+\Sigma^+$

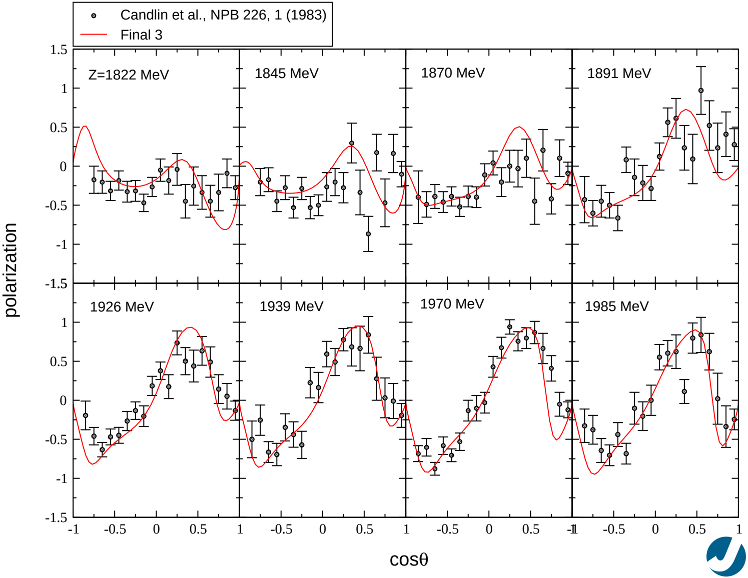

Spin rotation parameter β of $\pi^+ p \to K^+\Sigma^+$

Definitions Observabbles

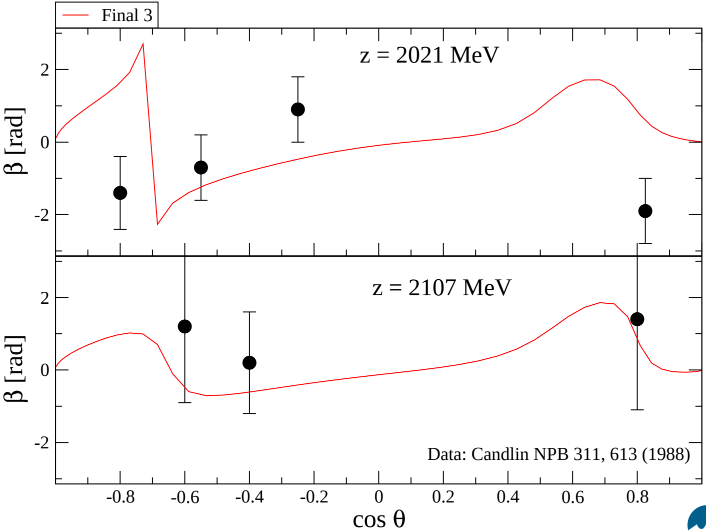

$\pi N \to \pi N$ phase shifts

Simultaneous fit to $\pi^+ p \to K^+ \Sigma^+$

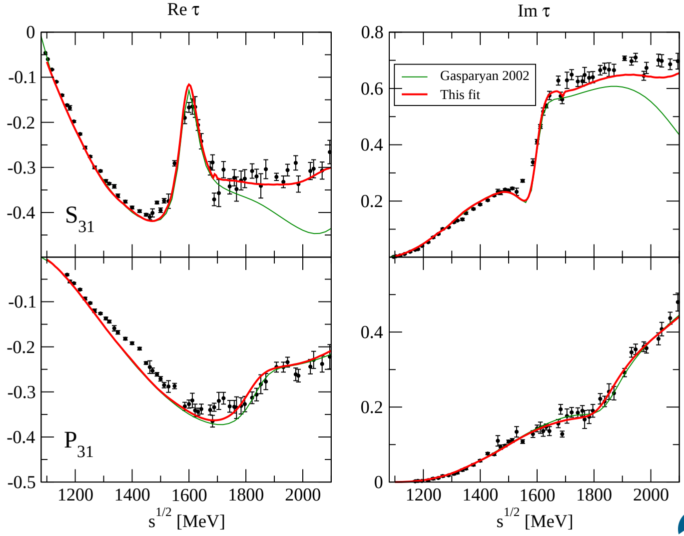

$\pi N \to \pi N$ phase shifts

Simultaneous fit to $\pi^+ p \to K^+ \Sigma^+$

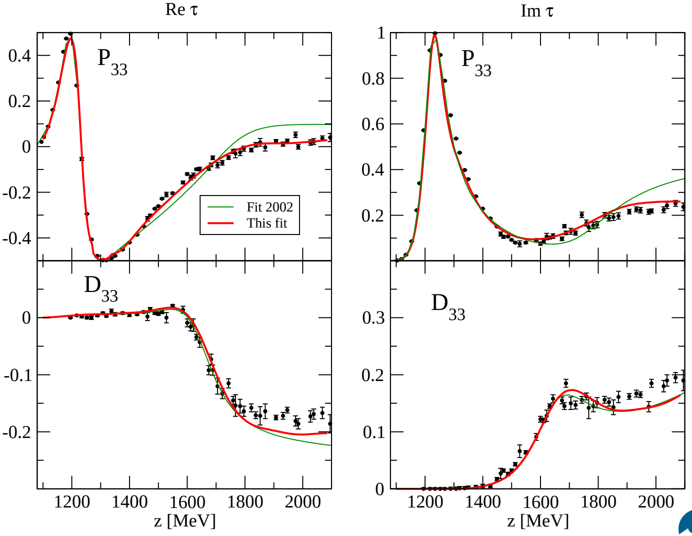

$\pi N \to \pi N$ phase shifts

New isospin 1/2, Spin 5/2 resonances (not needed for $\pi^+ p \to K^+ \Sigma^+$)

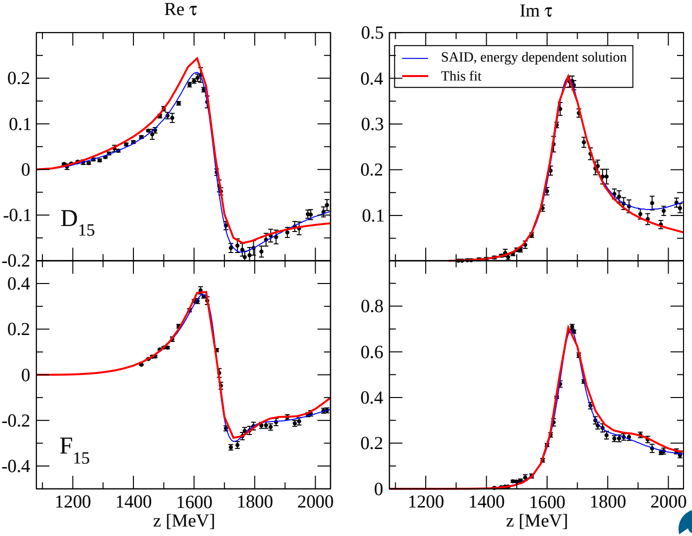

$\pi N \to \pi N$ phase shifts

Simultaneous fit to $\pi^+ p \to K^+ \Sigma^+$

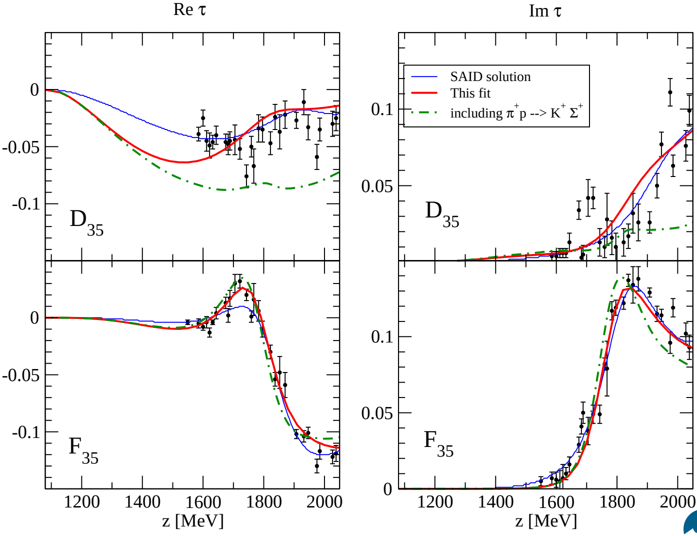

$\pi N \to \pi N$ phase shifts

Simultaneous fit to $\pi^+ p \to K^+ \Sigma^+$

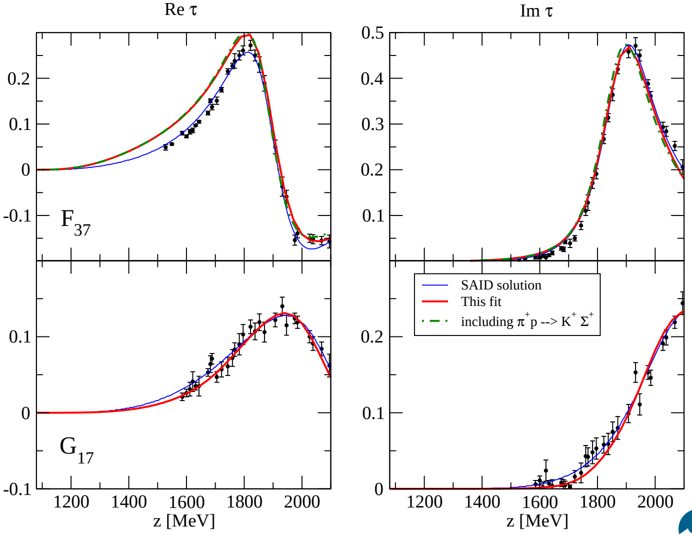

Comparison to Partial wave amplitudes of Candlin 1984

(Comparable quality of the fit)

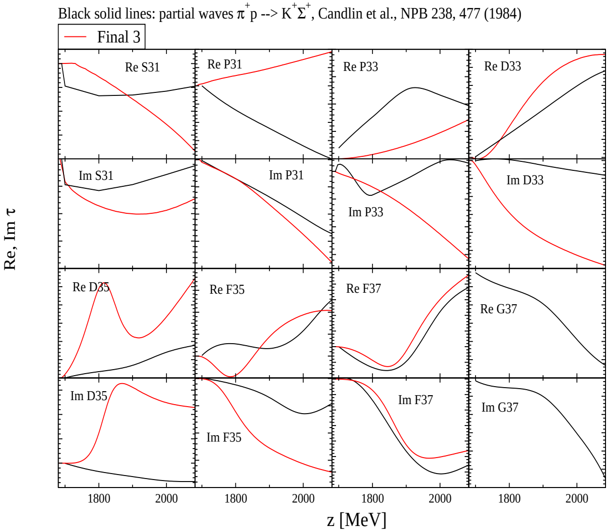

- Very different partial wave content!
- Additional constraints from $\pi N \to \pi N$ indeed necessary.
- New $P33$ and $S31$ states put in fit: Rather simulate some background than required as resonances.
- but pole extraction still to be done.

Conclusions

- Lagrangian based, field theoretical description of exchange processes $\rightarrow$ heavy constraints on the “background” (all partial waves are linked).
- Analyticity (real parts of loops) is important.
- Analytic continuation: precise, model independent determination of resonance parameters (poles).
- New developments: Chiral σ provides good description of $P11$. $P11$: Genuine, renormalized nucleon pole, dynamical Roper (mainly σN), dynamical P11(1620) (mainly $\pi\Delta$).
- Inclusion of KY channels and spin $5/2$, $7/2$ resonances.
- Combined description of $\pi N \rightarrow \pi N$ phase shifts and the $\pi^+ p \rightarrow K^+\Sigma^+$ reaction.
- Thank you for the invitation to this workshop!

Couplings " $g = \sqrt{a_{-1}}$ " to other channels

back

	$N\pi$	$N\rho^{(1)}$ $(S=1/2)$	$N\rho^{(2)}$ $(S=3/2)$	$N\rho^{(3)}$ $(S=3/2)$
$N^*(1535)\,S_{11}$	S_{11} $8.1+0.5i$	S_{11} $2.2-5.4i$	$-$	D_{11} $0.5-1.3i$
$N^*(1650)\,S_{11}$	S_{11} $8.6-2.8i$	S_{11} $0.9-9.1i$	$-$	D_{11} $0.3-2.0i$
$N^*(1440)\,P_{11}$	P_{11} $11.2-5.0i$	P_{11} $-1.3+3.2i$	P_{11} $3.6-2.6i$	$-$
$\Delta^*(1620)\,S_{31}$	S_{31} $2.9-3.7i$	S_{31} $0.0-0.0i$	$-$	D_{31} $0.0+0.5i$
$\Delta^*(1910)\,P_{31}$	P_{31} $1.2-3.5i$	P_{31} $0.2-0.4i$	P_{31} $-0.2-0.4i$	$-$
$N^*(1720)\,P_{13}$	P_{13} $3.7-2.6i$	P_{13} $0.1+0.8i$	P_{13} $-1.1+0.1i$	F_{13} $0.1+0.4i$
$N^*(1520)\,D_{13}$	D_{13} $8.4-0.8i$	D_{13} $-0.6+0.7i$	D_{13} $0.9-2.0i$	S_{13} $-2.5-22.8i$
$\Delta(1232)\,P_{33}$	P_{33} $17.9-3.2i$	P_{33} $-1.3-0.8i$	P_{33} $-0.9-3.0i$	F_{33} $0.0-0.0i$
$\Delta^*(1700)\,D_{33}$	D_{33} $4.9-1.0i$	D_{33} $-0.2+0.9i$	D_{33} $-0.4-0.4i$	S_{33} $-0.1-0.9i$
	$N\eta$	$\Delta\pi^{(1)}$	$\Delta\pi^{(2)}$	$N\sigma$
$N^*(1535)\,S_{11}$	S_{11} $11.9-2.3i$	$-$	D_{11} $-5.9+4.8i$	P_{11} $-1.4-1.2i$
$N^*(1650)\,S_{11}$	S_{11} $-3.0+0.5i$	$-$	D_{11} $4.3+0.4i$	P_{11} $-2.1-1.0i$
$N^*(1440)\,P_{11}$	P_{11} $-0.1+0.0i$	P_{11} $-4.6-1.7i$	$-$	S_{11} $-8.3-27.7i$
$\Delta^*(1620)\,S_{31}$	$-$	$-$	D_{31} $11.1-4.0i$	$-$
$\Delta^*(1910)\,P_{31}$	$-$	P_{31} $15.0-0.3i$	$-$	$-$
$N^*(1720)\,P_{13}$	P_{13} $-7.7+5.5i$	P_{13} $-14.1+3.0i$	F_{13} $0.0-0.3i$	D_{13} $-0.8+0.4i$
$N^*(1520)\,D_{13}$	D_{13} $0.16-0.60i$	D_{13} $0.0+0.4i$	S_{13} $-12.9-0.7i$	P_{13} $-0.6-0.6i$
$\Delta(1232)\,P_{33}$	$-$	P_{33} $-(4 \text{ to } 5)+i(0 \text{ to } 0.5)$	F_{33} ~ 0	$-$
$\Delta^*(1700)\,D_{33}$	$-$	D_{33} $-0.7-0.3i$	S_{33} $-19.7+4.5i$	$-$

Resonance couplings g_i $[10^{-3}\,\mathrm{MeV}^{-1/2}]$ to the coupled channels i. Also, the LJS type of each coupling is indicated. For the ρN channels, the total spin S is also indicated.

JÜLICH FORSCHUNGSZENTRUM

Zeros and branching ratio to πN, ηN

back

first sheet		second sheet		[FA02]
P_{11}	$1235 - 0\,i$	S_{11}	$1587 - 45\,i$	$1578 - 38\,i$
D_{33}	$1396 - 78\,i$	S_{31}	$1585 - 17\,i$	$1580 - 36\,i$
		P_{31}	$1848 - 83\,i$	$1826 - 197\,i$
		P_{13}	$1607 - 38\,i$	$1585 - 51\,i$
		P_{33}	$1702 - 64\,i$	–
		D_{13}	$1702 - 64\,i$	$1759 - 64\,i$

Position of zeros of the full amplitude T in [MeV]. [FA02]: Arndt et al., PRC 69 (2004).

	$\Gamma_{\pi N}/\Gamma_{\rm Tot}$ [%]	$\Gamma_{\eta N}/\Gamma_{\rm Tot}$ [%]
$N^*(1535)\,S_{11}$	48 [33 to 55]	38 [45 to 60]
$N^*(1650)\,S_{11}$	79 [60 to 95]	6 [3 to 10]
$N^*(1440)\,P_{11}$	64 [55 to 75]	0 [0 ± 1]
$\Delta^*(1620)\,S_{31}$	34 [20 to 30]	–
$\Delta^*(1910)\,P_{31}$	11 [15 to 30]	–
$N^*(1720)\,P_{13}$	13 [10 to 20]	38 [4 ± 1]
$N^*(1520)\,D_{13}$	67 [55 to 65]	0.10 [0.23 ± 0.04]
$\Delta(1232)\,P_{33}$	100 [100]	–
$\Delta^*(1700)\,D_{33}$	13 [10 to 20]	–

Branching ratios into πN and ηN. The values in brackets are from the PDG, [Amsler et al., PLB 667 (2008)].

JÜLICH FORSCHUNGSZENTRUM

Couplings and dressed vertices

Residue a_{-1} vs. dressed vertex Γ vs. bare vertex γ.

back

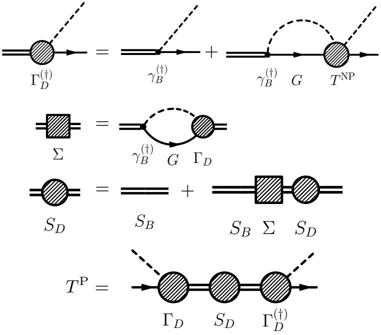

$$
\begin{aligned}
a_{-1} &= \frac{\Gamma_d\,\Gamma_d^{(\dagger)}}{1-\frac{\partial}{\partial Z}\Sigma} \\
g &= \sqrt{a_{-1}} \\
r &= |(\Gamma_D-\gamma_B)/\Gamma_D|, \\
r' &= |1-\sqrt{1-\Sigma'}|,
\end{aligned}
$$

- Dressed Γ depends on $T^{\rm NP}$.
- $\boxed{\sqrt{a_{-1}} \neq \Gamma \neq \gamma}$

	γ^C	Γ^C	r [%]	r' [%]
$N^*(1520)\,D_{13}$	$6.4-0.6i$	$13.2+1.2i$	53	61
$N^*(1720)\,P_{13}$	$-0.1+5.4i$	$0.9+4.8i$	24	45
$\Delta(1232)\,P_{33}$	$1.3+13.0i$	$-2.8+22.2i$	45	40
$\Delta^*(1620)\,S_{31}$	$0.1+14.3i$	$5.0+5.7i$	130	66
$\Delta^*(1700)\,D_{33}$	$5.4-0.8i$	$6.7+1.0i$	33	54
$\Delta^*(1910)\,P_{31}$	$9.4+0.3i$	$1.9-3.2i$	222	22

JÜLICH FORSCHUNGSZENTRUM

Pole repulsion in P_{33}

back

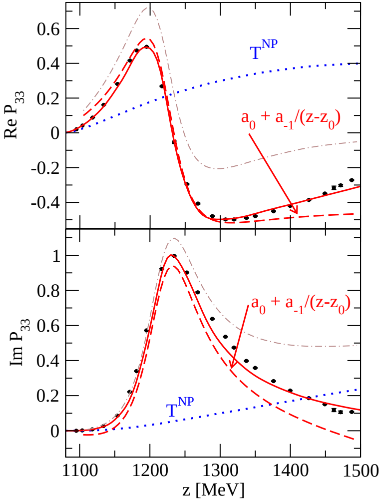

- Poles in T^{NP} may occur $\Rightarrow$ pole repulsion in $T = T^{\mathrm{NP}} + T^{\mathrm{P}}$!

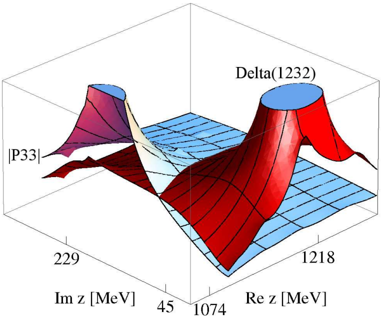

The D_{13} partial wave

back

The $N^*(1520)$ and a dynamically generated pole in T^{NP}.

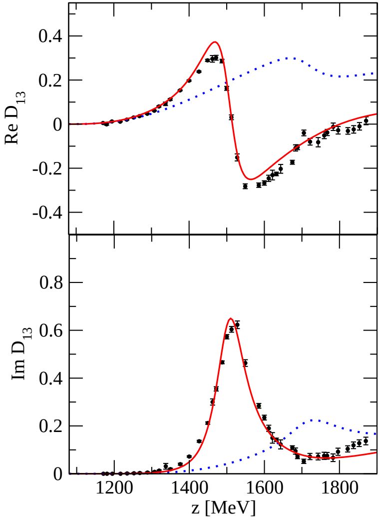

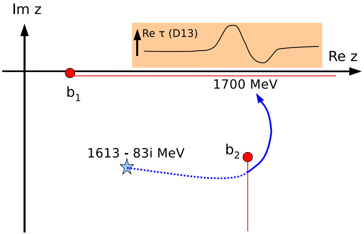

- T^{NP}: no s-channel $N^*(1520)$.
- Pole in T^{NP} on 3rd ρN sheet.
- On physical axis visible through branch point b_2.
- Pole invisible in full solution. $\rightarrow$ We do not identify it with a dynamically generated $N^*(1700)$.

[Ramos, Oset, arXiv:0905.0973 [hep-ph]]

Observables

back

g_{fi} und h_{fi} in JLS-Basis:

$$
\begin{aligned}
g_{fi} &= \frac{1}{2\sqrt{k_f k_i}} \sum_j (2j+1) d^j_{\frac{1}{2}\frac{1}{2}}(\theta) \left[\tau^{j(j-\frac{1}{2})\frac{1}{2}} + \tau^{j(j+\frac{1}{2})\frac{1}{2}}\right] \cos\frac{\theta}{2} \\
&+ \frac{1}{2\sqrt{k_f k_i}} \sum_j (2j+1) d^j_{-\frac{1}{2}\frac{1}{2}}(\theta) \left[\tau^{j(j-\frac{1}{2})\frac{1}{2}} - \tau^{j(j+\frac{1}{2})\frac{1}{2}}\right] \sin\frac{\theta}{2}
\end{aligned}
$$

$$
\begin{aligned}
h_{fi} &= \frac{-i}{2\sqrt{k_f k_i}} \sum_j (2j+1) d^j_{\frac{1}{2}\frac{1}{2}}(\theta) \left[\tau^{j(j-\frac{1}{2})\frac{1}{2}} + \tau^{j(j+\frac{1}{2})\frac{1}{2}}\right] \sin\frac{\theta}{2} \\
&+ \frac{i}{2\sqrt{k_f k_i}} \sum_j (2j+1) d^j_{-\frac{1}{2}\frac{1}{2}}(\theta) \left[\tau^{j(j-\frac{1}{2})\frac{1}{2}} - \tau^{j(j+\frac{1}{2})\frac{1}{2}}\right] \cos\frac{\theta}{2}
\end{aligned}
$$

JÜLICH FORSCHUNGSZENTRUM

Observables

back

$$\frac{d\sigma}{d\Omega} = \frac{k_f}{k_i}(|g_{fi}|^2 + |h_{fi}|^2)$$

$$= \frac{1}{2k_i^2}\frac{1}{2}\cdot\left(\left|\sum_j(2j+1)(\tau^{j(j-\frac{1}{2})\frac{1}{2}} + \tau^{j(j+\frac{1}{2})\frac{1}{2}})\cdot d^j_{\frac{1}{2}\frac{1}{2}}(\Theta)\right|^2\right.$$

$$\left. + \left|\sum_j(2j+1)(\tau^{j(j-\frac{1}{2})\frac{1}{2}} - \tau^{j(j+\frac{1}{2})\frac{1}{2}})\cdot d^j_{-\frac{1}{2}\frac{1}{2}}(\Theta)\right|^2\right)$$

$$\vec{P}_f = \frac{2Re(g_{fi}h_{fi}^*)}{|g_{fi}|^2 + |h_{fi}|^2}\cdot\hat{n}$$

$$\beta = \arctan\left(\frac{2Im(h_{fi}^* g_{fi})}{|g_{fi}|^2 - |h_{fi}|^2}\right)$$